

Abnormal dynamic functional connectivity of amygdalar subregions in untreated patients with first-episode major depressive disorder

Lihua Qiu, MD, PhD;* Mingrui Xia, PhD;* Bochao Cheng, MD, PhD; Lin Yuan, MS; Weihong Kuang, MD; Feng Bi, MD, PhD; Hua Ai, PhD; Zhongwei Gu, MS; Su Lui, MD, PhD; Xiaoqi Huang, MD, PhD; Yong He, PhD;* Qiyong Gong, MD, PhD*

Published online first Apr. 10, 2018; subject to revision

Background: Accumulating evidence supports the concept of the amygdala as a complex of structurally and functionally heterogeneous nuclei rather than as a single homogeneous structure. However, changes in resting-state functional connectivity in amygdalar subregions have not been investigated in major depressive disorder (MDD). Here, we explored whether amygdalar subregions — including the laterobasal, centromedial (CM) and superficial (SF) areas — exhibited distinct disruption patterns for different dynamic functional connectivity (dFC) properties, and whether these different properties were correlated with clinical information in patients with MDD. **Methods:** Thirty untreated patients with first-episode MDD and 62 matched controls were included. We assessed between-group differences in the mean strength of dFC in each amygdalar subregion in the whole brain using general linear model analysis. **Results:** The patients with MDD showed decreased strength in positive dFC between the left CM/SF and brainstem and between the left SF and left thalamus; they showed decreased strength in negative dFC between the left CM and right superior frontal gyrus ($p < 0.05$, family-wise error-corrected). We found significant positive correlations between age at onset and the mean positive strength of dFC in the left CM/brainstem in patients with MDD. **Limitations:** The definitions of amygdalar subregions were based on a cytoarchitectonic delineation, and the temporal resolution of the fMRI was slow (repetition time = 2 s). **Conclusion:** These findings confirm the distinct dynamic functional pathway of amygdalar subregions in MDD and suggest that the limbic-cortical-striato-pallido-thalamic circuitry plays a crucial role in the early stages of MDD.

Introduction

Major depressive disorder (MDD) is a common affective disorder characterized by a persistent negative mood and selective deficits in cognitive, circadian and motor functioning. Previous research has implicated the amygdala in emotion processing in mood disorders, and the amygdalo-striato-pallido-thalamic loop may play an important role in MDD.¹ The amygdala, which is closely interconnected with the cortical and subcortical brain regions, is a key hub for processing threats and orchestrating the complex set of emotional and physiologic responses² that underlie multidomain cognitive functions. In particular, the amygdala plays a central role in diverse cognitive-emotional interactions.³ Over the past decade, various neuroimaging studies have demonstrated structural and functional changes in the

amygdala of patients with MDD. Structural studies have found that altered amygdala volumes are state-related throughout the course of depression. For example, the volume of the amygdala was enlarged in first-episode, medication-naïve patients with MDD but decreased in patients with chronic MDD, due to neurotoxic effects.⁴⁻⁶ Functionally, abnormal brain activity in the amygdala has been widely reported in MDD, and these impairments may be associated with the excessive negative introspection and maladaptive rumination (e.g., brooding) observed in these patients.^{7,8} In addition, impaired resting-state amygdala-hippocampal/brainstem and amygdala-precuneus functional connectivity (FC) has recently been reported in adolescents with MDD, and negatively correlated with general depression, dysphoria and lassitude.⁹ Furthermore, reduced amygdalar connectivity with the dorsolateral prefrontal cortex,

Correspondence to: Yong He, PhD, Beijing Normal University, State Key Laboratory of Cognitive Neuroscience and Learning, IDG/McGovern Institute for Brain Research, Beijing Key Laboratory of Brain Imaging and Connectomics, 19 Xijiekouwai Street, Haidian District, Beijing, China; yong.he@bnu.edu.cn; Qiyong Gong MD, PhD, Huaxi MR Research Center, Department of Radiology, West China Hospital of Sichuan University, Chengdu, Sichuan, China; qiyonggong@hmrcc.org.cn

*These authors contributed equally to the work.

Submitted June 12, 2017; Revised Sept. 20, 2017; Revised Nov. 12, 2017; Accepted Nov. 17, 2017

DOI: 10.1503/jpn.170112

ventromedial prefrontal cortex and ventrolateral prefrontal cortex has been reported in depressed adolescents, and greater positive resting-state FC between the amygdala and insula is associated with a greater reduction in depression severity over time.¹⁰ Notably, previous studies have focused on amygdalar FC, which usually estimates stationary synchronization between brain regions during the entire scan period but ignores its dynamic, time-varying characteristics. Researchers have recently applied newly developed dynamic FC (dFC) analysis strategies to investigate neuropsychiatric diseases such as Alzheimer disease¹¹ and schizophrenia,¹² and provided novel understandings of their pathology. Previous studies have also demonstrated altered dFC variability in the medial prefrontal cortex (mPFC)¹³ and large-scale functional networks¹⁴ in patients with MDD. However, little is known about abnormal dFC in the amygdalae of patients with MDD.

Most neuroimaging studies of patients with MDD have considered the amygdala as a single homogeneous structure. For example, decreased FC has been identified in the amygdala, frontal cortex, supplementary motor area (SMA), thalamus and hippocampus in medication-naïve adults with first-episode MDD.¹⁵ Impaired amygdala FC has also been found in adults with late-life depression¹⁶ and adolescents with MDD.⁹ However, increasing evidence suggests that the amygdala is a complex of structurally and functionally heterogeneous nuclei rather than a single homogeneous structure. Based on the cytoarchitectonic characteristics of the amygdala, Amunts and colleagues¹⁷ suggested that it can be divided into the following major subregions: the laterobasal (LB), centromedial (CM) and superficial (SF) nuclei. Furthermore, tractography,¹⁸ task-based¹⁹ and resting-state functional MRI (fMRI)^{20,21} studies of healthy adults have revealed distinct connectivity profiles and unique functions for these 3 subregions. The LB region receives inputs from the auditory system, specifically the thalamic and cortical stations, which are both involved in conditioned stimulus transmission.²² Neurons in the LB nuclei encode fear memories related to these sensory stimuli, signal the threat value of a stimulus and modulate memory encoding and sensory processing in other brain regions.^{22,23} The CM subregion, which is composed of the central and medial nuclei, may play an important role in generating behavioural responses. The central nucleus achieves these functions through projections to the brainstem, hypothalamic and striatal regions and basal forebrain targets.^{23,24} The SF nuclei adjacent to the LB region have extensive bilateral connections with the olfactory cortex, insular cortex, ventral striatum/nucleus accumbens and hippocampus/parahippocampal gyrus,^{25,26} which are involved in the detection of emotionally salient stimuli and the processing of socially relevant information, including olfactory and emotional stimuli.²⁷ In humans, the SF nuclei are implicated in the processing of socially relevant information and the modulation of approach-avoidant behaviour.¹⁹

Abnormalities in amygdala subregion-based networks have been found in attention deficit-hyperactivity disorder,²⁸ generalized anxiety disorder,^{20,29} unilateral temporal epilepsy³⁰ and autism-spectrum disorder³¹; however, very few studies investigate amygdala dysfunction at the subregional level. Whether the resting-state FC of amygdalar subregions

is disrupted in patients with MDD remains largely unknown. More importantly, dFC analysis can capture fluctuation in resting-state FC over a very short period, which could provide abundant information about the time-varying functional architecture of specific regions. Exploring MDD-relevant abnormalities in the dFC properties of the amygdalar subregions could help to determine the disruptions in functional organization that underlie the clinical symptoms of MDD — disruptions that cannot be detected by static FC analysis.

In this study, we collected resting-state fMRI data from 31 patients with first-episode MDD and 64 matched controls to study the abnormal dFC in amygdalar subregions. These patients were untreated to exclude the potential influence of attack frequency, medication or other therapeutic methods on the amygdala-related network. We calculated the whole-brain dFC of each amygdalar subregion using the sliding-window method. Then, we determined between-group differences in the mean strength and variance of the dFC using 2-sample *t* tests. We also examined correlations between the dFC properties of regions that exhibited significant between-group differences and clinical findings. Given that previous studies have revealed distinct abnormal FC patterns in the amygdalar subregions^{20,28–31} and demonstrated associations between subregional FC and clinical symptoms in neuropsychiatric disease,^{28,30,31} we hypothesized that the subregions of the amygdala would exhibit distinct disruptions in dFC properties among patients with MDD, and that the disrupted dFC might be related to clinical findings in MDD.

Methods

Participants

We initially recruited 31 first-episode, drug-naïve patients with MDD (18–60 years old) and 64 age- and sex-matched healthy controls (16–81 years old) via the Mental Health Centre of West China Hospital, Chengdu, China. We removed 1 patient and 2 controls because of excessive head motion (see Image preprocessing). Diagnoses of MDD and duration of illness were determined by consensus between the attending psychiatrist and a trained interviewer using the Structured Clinical Interview (SCID), patient version, from the *Diagnostic and Statistical Manual of Mental Disorders*, fourth edition (DSM-IV).³² We assessed the presence of psychiatric illness in first-degree relatives based on the descriptions of the patient or his/her family. None of the controls had a history of psychiatric illness as determined by the SCID nonpatient interviews or known psychiatric illnesses in first-degree relatives. Depression severity was rated in patients using the 17-item Hamilton Depression Rating Scale.³³ All patients scored at least 18 on the 17-item scale on the day of the MRI examination. None of the participants had previously received psychotropic medication or psychotherapy. The duration between the first illness manifestation (i.e., when the patient presented with depressive symptoms for the first time — not the diagnosis) and MRI ranged from 2 to 60 weeks. Potential participants were excluded if they had significant systemic or neurologic illness. Two experienced radiologists determined that all participants were free of abnormalities on con-

ventional MRI. The Ethical Committee of the West China Hospital of Sichuan University approved this study, and written informed consent was obtained from all participants.

Image acquisition

All participants were scanned using a 3 T MRI system (EXCITE; General Electric, 8-channel head-coil). During the scans, participants were instructed to remain still, keep their eyes closed and not think of anything in particular. We obtained resting-state fMRI images using a gradient-echo echo-planar imaging sequence with the following parameters: repetition time 2000 ms, echo time 30 ms, flip angle 90°, 30 slices, slice thickness 5 mm, field of view 240 × 240 mm², matrix 64 × 64, voxel size 3.75 × 3.75 × 5 mm³. Each scan lasted 400 s (i.e., 200 volumes).

Image preprocessing

We performed image preprocessing using the SPM8 package (www.fil.ion.ucl.ac.uk/spm) and DPARSF.³⁴ The first 5 volumes for each participant were discarded because of signal equilibrium and the participant's adaptation to the scanning environment. The remaining images were corrected for acquisition time intervals between slices and head motion between volumes. Data from 1 patient and 2 control participants were discarded because their head motion exceeded 3 mm of translation or 3° of rotation in any direction. Following these corrections, images were spatially normalized to the standard Montreal Neurological Institute space, resampled into 3 mm isotropic voxels and spatially smoothed with a Gaussian kernel (full width at half maximum 4 mm). Linear detrend and band-pass filtering (0.01 to 0.08 Hz) were performed to reduce the effects of low-frequency drift and high-frequency noise. Then, several nuisance signals — including the Friston-24 head motion parameters,³⁵ global mean and noise from cerebrospinal fluid and white matter — were regressed out of the data.

Definition of amygdalar subregions

We defined 3 amygdalar subregions in each hemisphere using cytoarchitectonically defined probabilistic maps from the JuBrain Cytoarchitectonic Atlas³⁶ as implemented in the SPM Anatomy Toolbox (www.fz-juelich.de/inm/inm-1/DE/Forschung/_docs/SPMANatomyToolbox/SPMANatomyToolbox_node.html).³⁷ Voxels were included as potential amygdalar subregions only when the probability of their assignment to the amygdalar subregion was higher (likelihood greater than 40%) than that of assignment to other nearby structures. Each voxel was exclusively assigned to a single region, resulting in the following, non-overlapping amygdalar subregions in each hemisphere: CM, LB and SF.¹⁷ These subregions were considered to be the seeds for further FC analyses.

Resting-state dFC analysis

To obtain the whole-brain resting-state dFC map of each seed, we used a common sliding-window approach for each participant.^{38,39} Briefly, we cropped 195 preprocessed volumes of data

into time windows of 100 volumes and slid the window 1 volume at a time, as follows: 1–100, 2–101, etc., and 96–195, yielding 96 time windows in total. Within each sliding window, the whole-brain FC maps for each amygdalar subregion were computed as the Pearson correlation coefficient between the averaged time course of all voxels in the seed and the time course of every other voxel in the grey matter. The resulting correlation coefficients were converted to z-scores using Fisher *r*-to-*z* transformation to improve normality. Therefore, we obtained 96 z-score maps for each participant, representing the whole-brain dFC fluctuation for each amygdalar subregion.

Two metrics were estimated to capture the strength and variability of the dFC. Mean strength was calculated by averaging the 96 dFC z-score maps. Variability was calculated as the variance of the 96 z-scores at each voxel. Therefore, for each participant, we also obtained voxelwise mean strength and variance maps for the dFC with respect to each amygdalar subregion.

Statistical analysis

To examine the within-group FC patterns of each amygdalar subregion for the MDD and control groups, we performed 1-sample *t* tests on the individual mean strength maps for each amygdalar subregion. As suggested in a recent study investigating the ability of statistical methods to control false-positive rates in fMRI studies,⁴⁰ we strictly controlled the false-positive rate in our imaging statistics by setting the statistical significance threshold to $p < 0.001$ at the voxel level, and a family-wise error (FWE)-corrected value of $p < 0.05$ at the cluster level using SPM. The FWE correction in SPM is commonly used for multiple comparison correction based on random-field theory, which works by calculating the smoothness of the statistic image and estimating the likelihood of clusters with particular statistic levels occurring by chance. The statistics were constrained within a grey matter mask, generated by setting a threshold of 0.2 on the grey matter probability map provided in the SPM8 toolbox.

To assess between-group differences in the mean strength and variance values of the dFC in each amygdalar subregion, we used a general linear model (dependent variable, dFC metrics; independent variable, group), with age and sex as covariates. The significance threshold was set to $p < 0.001$ at the voxel level, and FWE correction at the cluster level to $p < 0.05$. Between-group differences were determined by the significant clusters that belonged to the significant within-group connectivity maps for one or both groups. Computations for positive and negative FC were performed separately.

To determine whether dFC abnormalities were associated with clinical indicators (i.e., age at onset, illness duration and Hamilton Depression Rating Scale score), we performed general linear models with the clinical indicators as the dependent variables, dFC metrics as the independent variable and age and sex as covariates. Because only some of the patients' symptoms were recorded, we did not calculate the relationship between dFC abnormalities and symptom dimensions. We performed these analyses in the regions that showed a significant between-group difference. The significance threshold was set to the FWE-corrected $p < 0.05$.

Validation

To validate the reliability of our major results, we examined the influences of different image-preprocessing and data-analysis strategies as follows. First, given that many of the patients with MDD were female, we conducted the primary analyses again with women only. Second, previous studies have suggested that global signal regression can reduce the effects of non-neuronal activity such as respiration,^{41–43} while simultaneously introducing widespread negative FC with ambiguous biological interpretations.^{44,45} Thus, we repeated our analysis without global signal regression in the data preprocessing. Third, to compare the differences in findings between dFC and traditional static FC analyses, we also performed static FC analysis for each amygdalar subregion using the entire time series. Fourth, to assess whether our findings from using the amygdala subregions as seeds could also be detected using the whole amygdala as a region of interest, we re-performed our analysis combining the 3 amygdalar subregions as a single seed. Fifth, several recent resting-state fMRI studies have reported the influence of head motion on FC.^{46–49} Neither maximum translation nor maximum rotation revealed significant differences between the patient and control groups (both $p > 0.63$); however, we did find that the mean framewise displacement⁴⁷ differed between the 2 groups ($p = 0.03$). Because the “scrubbing” procedure would create inconsistent time point lengths across different participants by deleting volumes or introduce artificial signals into the time series by interpolating volumes — reducing the credibility of the dFC analysis — we did not perform this procedure on the preprocessed images. Rather, we re-performed the between-group general linear model tests on the dFC metrics by adding framewise displacement as a covariate to reduce the motion effect. We used the general linear model analyses to explore the association between abnormalities in dFC variance and clinical indicators, with age and sex as covariates. Finally, we used a common sliding-window approach to capture the dynamics of FC,^{11,38,39,50,51} but the choice of window length remains contro-

versial. Our main analyses used a sliding window with a length of 200 s to capture the primary low-frequency blood oxygen level-dependent signal fluctuations. We used 2 additional window lengths (160 s and 240 s) to validate the main results.

Results

Demographic and neuropsychological tests

Demographic characteristics are shown in Table 1. We observed no significant differences between the MDD and control groups with respect to sex or age (both $p > 0.06$).

Within-group dFC patterns of amygdalar subregions

The main results reported below were based on the dFC analysis using 100 volumes (200 s) as the window length. The results of the 2 additional window lengths (160 s and 240 s) are reported in Appendix 1, available at jpn.ca/170112-a1. The within-group analysis revealed a similar spatial mean dFC pattern of the bilateral amygdalar subregions in the MDD and control groups; however, visual examination indicated that the strength and scope of the mean dFC in the MDD group were less than those in the control group (mean T values of the significant clusters: positive dFC = 6.106–6.624 for controls, 5.350–5.686 for MDD; negative dFC = 4.508–4.925 for controls, 4.042–4.604 for MDD. Total cluster size: positive dFC = 334 611–395 901 mm³ for controls, 135 648–220 347 mm³ for MDD; negative dFC = 260 280–318 168 mm³ for controls, 39 771–135 729 mm³ for MDD). In both groups, the positive mean dFC of the bilateral amygdalar subregions was primarily connected to the temporal lobe, sensorimotor cortex and subcortical areas of the brain, as well as the caudate, putamen, thalamus, brainstem and cerebellum. The negative mean dFC of the bilateral amygdalar subregions was primarily connected to the frontal-parietal and occipital lobes (Fig. 1).

Table 1: Participant demographic and clinical characteristics

Characteristic	All participants; mean ± SD (range)*			Female participants; mean ± SD (range)*		
	MDD (n = 30)	Control (n = 62)	p value	MDD (n = 22)	Control (n = 33)	p value
Age, yr	36.1 ± 12.3 (18–60)	35.1 ± 15.9 (16–81)	0.77†	37.5 ± 11.5 (20–57)	36.5 ± 15.2 (18–73)	0.78†
Sex, male:female	8:22	29:33	0.065‡	0:22	0:33	NA
Education, yr	3.8 ± 1.4 (1–6)	NA		3.7 ± 1.4 (1–6)	NA	
Duration, wk	16 ± 14.1 (2–60)	NA		13.5 ± 11.4 (2–36)	NA	
HDRS score	24.3 ± 5.0 (18–34)	NA		24.0 ± 4.6 (18–34)	NA	
Onset age, yr	35.8 ± 12.2 (18–59)	NA		37.3 ± 11.5 (20–56)	NA	
Head motion, mean FD	0.09 ± 0.05 (0.03–0.23)	0.12 ± 0.05 (0.05–0.35)	0.03†	0.09 ± 0.05 (0.03–0.23)	0.12 ± 0.07 (0.05–0.35)	0.04†
Head motion, max translation	0.44 ± 0.34 (0.13–1.66)	0.47 ± 0.38 (0.07–2.40)	0.63†	0.48 ± 0.38 (0.13–1.66)	0.44 ± 0.26 (0.15–1.11)	0.65†
Head motion, max rotation	0.62 ± 0.53 (0.06–2.66)	0.65 ± 0.61 (0.10–2.93)	0.85†	0.67 ± 0.57 (0.13–2.66)	0.61 ± 0.59 (0.12–2.93)	0.72†

FD = framewise displacement; HDRS = Hamilton Depression Rating Scale; MDD = major depressive disorder; NA, not applicable; SD = standard deviation.

*Unless indicated otherwise.

†Obtained using 2-sample t test.

‡Obtained using Pearson χ^2 test.

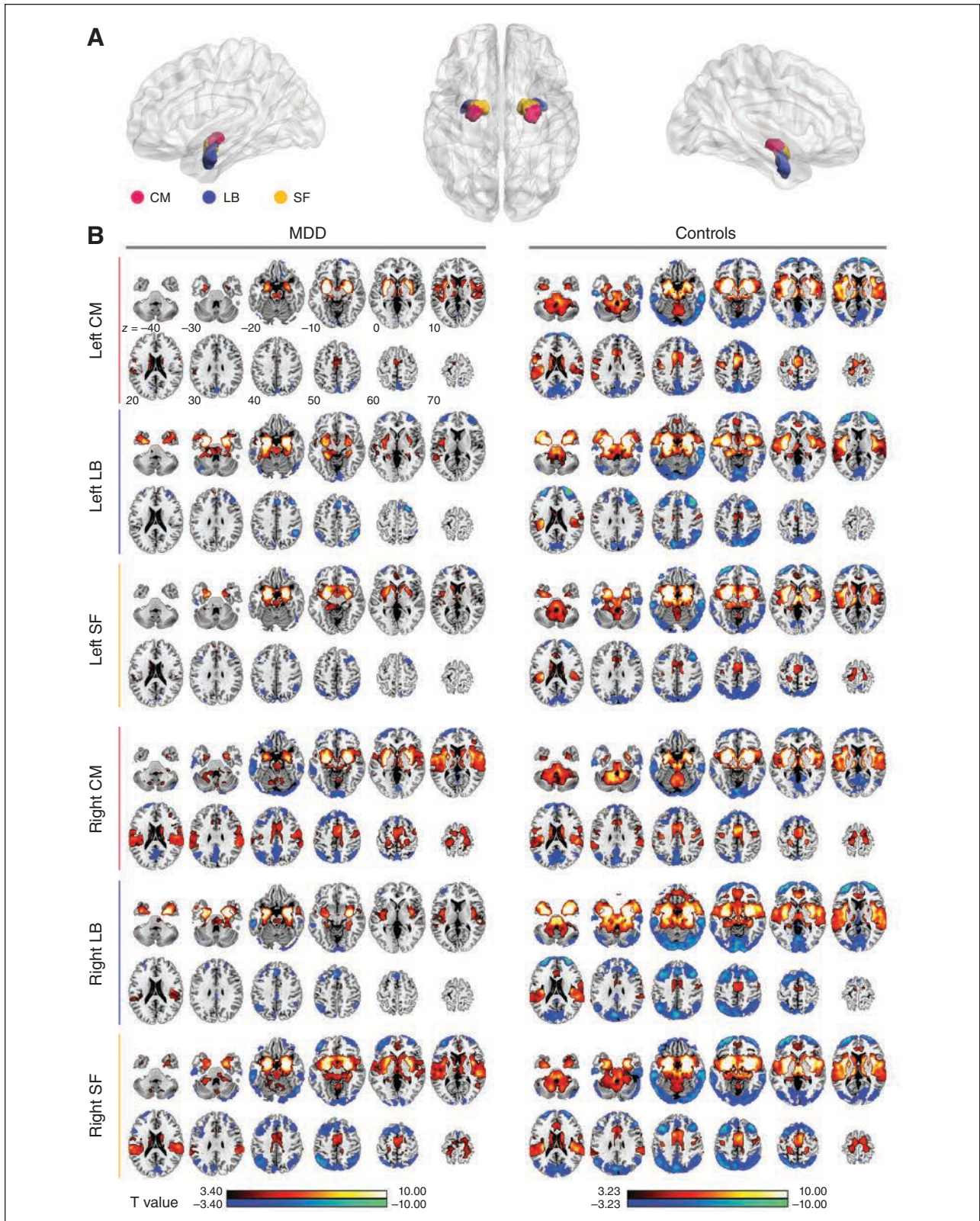


Fig. 1: The mean dynamic functional connectivity (dFC) map of each amygdalar subregion in each group. **(A)** The subregions of the amygdala: the centromedial (CM; magenta), laterobasal (LB; blue) and superficial (SF; yellow). **(B)** The mean dFC map of each amygdalar subregion in the major depressive disorder (MDD) and control groups. Warm colours indicate positive mean connectivity and cool colours represent negative mean connectivity.

Between-group differences in amygdalar subregional dFC properties

Differences in strength of positive dFC

Compared with the controls, patients with MDD showed decreased positive mean dFC of the left CM and SF regions, primarily in the brainstem, and decreased positive mean dFC between the left SF region and left thalamus, primarily in the mediodorsal thalamic nucleus ($p < 0.05$, FWE-corrected, Fig. 2). In addition, patients with MDD also showed a trend toward decreased positive mean dFC between the right CM and brainstem ($p = 0.024$, uncorrected, Appendix 1, Figure S10). The detailed locations and sizes are listed in Table 2.

Differences in strength of negative dFC

Compared with the controls, patients with MDD showed decreased negative mean dFC of the left CM region with

respect to the right superior frontal gyrus (SFG; $p < 0.05$, FWE-corrected; Table 2 and Fig. 3).

Differences in dFC variability

The variability of the positive dFC between the left LB region and right SMA revealed a nonsignificant trend toward an increase in patients with MDD compared with that in the controls ($p = 0.01$, uncorrected). The variance of the positive dFC differences between the MDD and control groups is presented in Table 2 and Appendix 1, Figure S10.

Correlation between dFC properties and clinical variables in patients with MDD

The mean positive dFC strength between the left CM region and brainstem was positively correlated with the age of MDD onset in the MDD group ($r = 0.59$, $p = 0.026$, FWE-corrected).

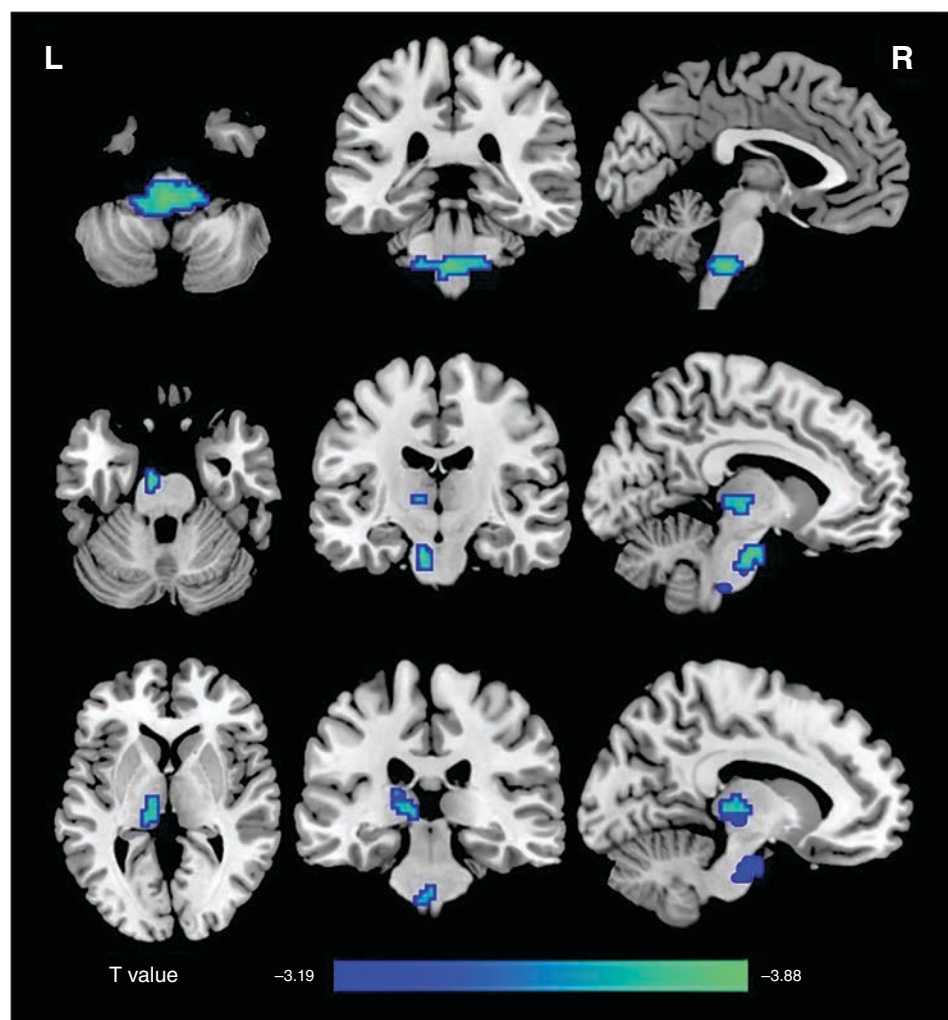


Fig. 2: Group differences in the mean positive strength of dynamic functional connectivity (dFC) in amygdalar subregions. Compared with the control group, the major depressive disorder group showed a decreased positive mean dFC between the left centromedial/superficial regions and the brainstem, as well as between the left superficial region and the left thalamus ($p < 0.05$, family-wise error-corrected). L = left; R = right.

Table 2: Regions showing significant between-group differences

Seed	Region	BA	Cluster size, mm ³	Peak MNI coordinates, x, y, z	t	p_{FWE} value
Positive mean dFC						
Left CM	Brainstem		2727	-3, -33, -45	-4.65	0.001
Right CM	Brainstem		999	-12, -51, -33	-3.99	0.08 (0.024*)
Left SF	Brainstem		1350	-9, -15, -27	-4.61	0.015
Left SF	Left thalamus		999	-12, -27, 3	-4.00	0.04
Negative mean dFC						
Left CM	Right SFG	10	1242	15, 66, 12	-4.46	0.048
Variance of positive dFC						
Left LB	Right SMA	6	351	3, -12, 63	4.11	0.085 (0.010*)

BA = Brodmann area; CM = centromedial; dFC = dynamic functional connectivity; FWE = family-wise error; MNI = Montreal Neurological Institute; LB = laterobasal; SF = superficial; SFG = superior frontal gyrus; SMA = supplementary motor area.

*Uncorrected cluster p value.

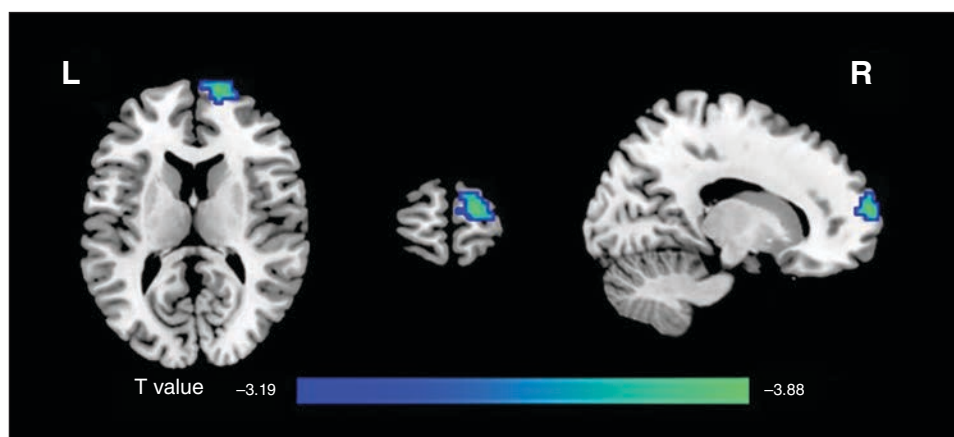


Fig. 3: Group differences in the mean negative strength of dynamic functional connectivity (dFC) in amygdalar subregions. The major depressive disorder group showed a decreased negative mean dFC between the left centromedial region and right superior frontal gyrus ($p < 0.05$, family-wise error-corrected). L = left; R = right.

Additionally, the mean positive dFC between the left SF region and brainstem revealed a trend toward a positive association with disease duration ($r = 0.56$, $p < 0.001$, uncorrected) and age of onset ($r = 0.54$, $p < 0.001$, uncorrected) in patients with MDD (Table 3 and Fig. 4).

Validation

To evaluate the reliability of our main findings, we reperformed our analyses using different analysis strategies. We found that the results mostly remained consistent, with slight changes in cluster significance in several conditions, including in only female participants, static FC analysis and different window length. We noticed that the results without global mean regression were quite different from the results with global signal regression. Specifically, the disrupted dFC was mainly between the left insula and bilateral LB and left SF, between the left LB and left orbital frontal cortex, and between the left SF and brainstem. This result might indicate mixed factors in the difference in dFC between patients with MDD and controls. Moreover, we found that the static analy-

sis showed some results similar to the mean dFC, such as connection of the left CM with the brainstem and SFG. However, dFC analysis revealed an additional difference in connectivity between the left SF and brainstem and thalamus, as well as dynamic fluctuation between the left LB and SMA, that could not be identified using static FC analysis. Interestingly, we found no significant between-group differences in the mean or variability of the dFC when using whole amygdala as seeds, suggesting the need to divide the amygdala into subregions. Details are presented in Appendix 1.

Discussion

To the best of our knowledge, this study was the first to investigate the whole-brain resting-state dFC of amygdalar subregions in untreated patients with first-episode MDD. Patients with MDD showed decreased strength in positive dFC between the left CM/SF and brainstem and between the left SF and left thalamus. As well, patients with MDD exhibited decreased strength in negative dFC between the left CM region and right SFG. Moreover, we found positive correlations

Table 3: dFCs showing significant correlations between dynamic properties and clinical variables

Seed	Region	Metric	Clinical variable	Peak MNI coordinates, <i>x, y, z</i>	<i>r</i>	<i>p</i> value	<i>p</i> _{FWE} value
Left CM	Brainstem	Mean dFC	Onset age	-21, -33, -45	0.59	< 0.001	0.026
Right CM	Brainstem	Mean dFC	HDRS	-9, -54, -30	0.49	0.006	0.08
Left SF	Brainstem	Mean dFC	Onset age	-6, -30, -45	0.54	0.002	0.09
Left SF	Brainstem	Mean dFC	Duration	-6, -30, -45	0.56	0.001	0.07

CM = centromedial; dFC = dynamic functional connectivity; FWE = family-wise error; HDRS = Hamilton Depression Rating Scale; MNI = Montreal Neurological Institute; SF = superficial.

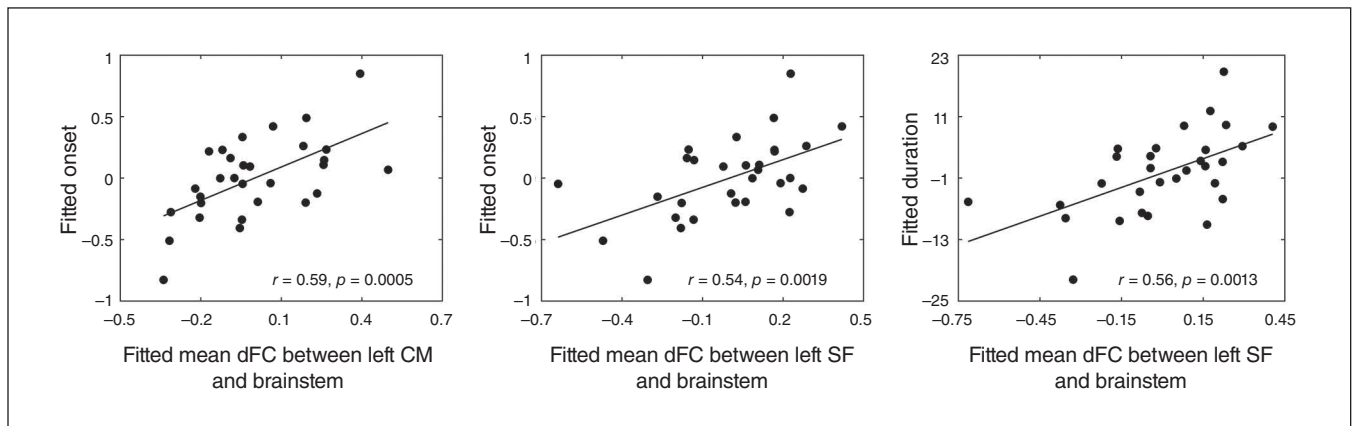


Fig. 4: The correlations between the dynamic functional connectivity (dFC) properties and clinical variables in patients with major depressive disorder. The mean dFC between the left centromedial (CM) region and the brainstem was positively correlated with age at onset. The mean dFC between the left superficial (SF) region and the brainstem was positively correlated with age at onset and disease duration.

between the mean positive dFC of the CM region and brainstem with respect to age of onset, suggesting that the CM region may play an important role in the initiation of MDD. Together, these results suggest a distinct disruption pattern in the subregions of the amygdala with respect to the dFC properties of patients with MDD and provide additional experimental evidence for understanding the functional disconnection in these patients.

Differences in positive mean dFC

The most unique finding of our study was the decreased positive mean dFC between the left CM/SF region and brainstem during the early stages of MDD. Previous studies have found that the CM region generates behavioural responses by projecting to the brainstem^{23,24} to control the expression of fear responses and modulate visceral function in relation to emotional stimuli,⁵² including freezing behaviours and related responses in the autonomic nervous (e.g., blood pressure and heart rate) and endocrine (pituitary-adrenal hormone) systems.⁵³ The SF subdivision of the amygdala is involved in olfactory^{52,54} and affective processing.^{55,56} The brainstem is the major region that innervates neurotransmitter release to the hypothalamic-pituitary-adrenal axis and frontolimbic circuits, key brain circuits in patients with MDD.⁵⁷ Consistent with our results, a significant and specific decrease in the white matter integrity of the right solitary

tract that connects the brainstem to the amygdala has also been found in participants with MDD.⁵⁷ Impaired amygdala-brainstem circuits assessed using resting-state fMRI FC analysis have been reported only in adolescents with MDD.⁹ Our results demonstrate that impaired amygdala-brainstem circuits are not unique to adolescents with MDD. However, we found no significant between-group differences in the mean or variability of the dFC by using the whole amygdala as seeds (the detailed results are shown in Appendix 1). Because the 3 subregions of the amygdala have distinct connectivity profiles, the dFC change by using the whole amygdala as seeds might not be detected if the 3 subregions were altered in the inverse direction. Thus, it is necessary to divide the amygdala into subregions to detect subtle structural and functional changes. Combining the study of adolescents with MDD and the results of the current study, we speculate that the impaired amygdala-brainstem circuits are persistent from adolescence to adulthood, and that the CM/SF subregions play a key role in the amygdala-brainstem circuits.

In the current study, we found a modest positive correlation between the mean dFC strength of the left CM-brainstem and age at illness onset, as well as a trend toward a positive correlation between the dFC of the left SF-brainstem and disease duration. A previous study revealed that amygdala-brainstem connectivity is inversely correlated with general depression, dysphoria and lassitude; moreover, amygdala-brainstem connectivity is positively correlated

with well-being.⁹ However, only some of the patients' symptoms were recorded in the current study; therefore, we could not judge whether this connection was related to symptoms. Whether CM/SF-brainstem connectivity is a self-protective mechanism that delays the onset of disease or a compensatory response to maintain normal brain function requires further study to investigate the dynamic change between CM/SF-brainstem connectivity and clinical symptoms. Nevertheless, the present and previous results suggest that CM/SF-brainstem connectivity plays an important role in the pathophysiology of early-stage MDD.

In addition to the impaired positive mean dFC between the left CM/SF region and the brainstem, we found a reduced positive mean dFC between the left SF region and thalamus in untreated patients with first-episode MDD. In monkeys, anterograde and retrograde axonal tracing, as well as electrophysiological recording, revealed that the medial thalamic nucleus receives substantial subcortical inputs from the amygdala and other limbic areas.⁵⁸ Acute footshock in rats activates the paraventricular neurons of the thalamus that project to the mPFC, nucleus accumbens and amygdala,⁵⁹ demonstrating that the paraventricular nucleus of the thalamus responds to various stressors. Therefore, the hypoconnectivity between the SF region and thalamus in patients with MDD might be associated with consistent negative emotions in response to various stressors.

Differences in negative mean dFC

In addition to the impaired positive mean dFC, the negative mean dFC analysis revealed reduced connectivity strength between the CM region with respect to the SFG in patients with MDD. The SFG belongs to the medial prefrontal network, which modulates visceral function in relation to emotion or other factors. Previous fMRI studies have shown that activity in the mPFC correlates with visceral activation in response to emotional^{60,61} or even nonemotional⁶² stimuli. The most prominent connections of the amygdaloid are with areas of the medial network. Consistent with our results, a recent study of medication-naïve depressed adolescents showed reduced amygdala-based resting-state FC with the dorsolateral prefrontal cortex and ventromedial prefrontal cortex.¹⁰ Animal studies have also revealed negative FC between the amygdala and mPFC. In rats, stimulation of the amygdala inhibits neuronal ensemble activity in the mPFC, and stimulation of the mPFC to the amygdala excites intramygdaloid GABAergic cells that inhibit neuronal activity in the central amygdaloid nucleus.^{63,64} Thus, the hypoconnectivity between the CM region and SFG observed in the current study might be related to impaired roles in modulating visceral responses to stressors and emotional stimuli in patients with MDD.

Differences in variability

We observed a trend toward increased variability in the positive dFC of the left LB region with regard to the SMA in the MDD group. This variability in neural activity (i.e., standard

deviation [SD]), which is often considered a measurement-related confounding of blood oxygen level-dependent signals, is central to both resting-state and task-evoked activity in the healthy brain.^{65–67} Although the concept of variability has not completely eluded fMRI research, its intrinsic theoretical and predictive meaning is unclear; variance in these data are typically considered “noise,” but may represent a vital feature of brain function. Research in young and older adults revealed that the SD- and mean-based spatial patterns are essentially nonoverlapping.⁶⁵ Consistent with that study, our variability results with respect to the positive dFC also revealed a distinct brain region with mean positive dFC. McIntosh and colleagues⁶⁸ found that greater multi-channel electroencephalography (EEG) signal variability was highly correlated with a more consistent reaction time and more accurate performance, suggesting that moment-to-moment variability in brain activity is a critical index of cognitive capacity. Garrett and colleagues⁶⁵ also found that young adults exhibited higher variability overall, which may represent an “optimal” system (i.e., a “sophistication” or “coherence” argument). The current study adds to psychoradiology, a promising clinical radiology subspecialty focusing on psychiatric disorders.⁶⁹

Limitations

Several limitations must be addressed. First, although our study found dFC abnormalities in the amygdalar subregions of untreated patients with first-episode MDD, much remains unknown about whether these abnormalities exist across MDD subtypes and whether treatments for MDD affect dFC. Future imaging studies including patients with different subtypes of MDD and using longitudinal data before and after treatments (including medication, behaviour therapy or electroconvulsive therapy) would help to understand the pathophysiological mechanisms of MDD and provide potential biomarkers for the early diagnosis and optimal selection of therapeutic targets for MDD. Second, the definition of amygdalar subregions in the current study was based on a cytoarchitectonic delineation, and our results and those of previous studies have shown distinct FC patterns for each subregion. However, the exact relationship between the microscopic morphology and functions of amygdalar subregions remains largely unclear. Future studies should combine both cytoarchitectonic and functional imaging data to further understand the gap between microstructures and macrofunctions and provide novel divisions for the amygdala and other brain regions. Finally, the temporal resolution of commonly used fMRI techniques is approximately 2 s per volume (0.5 Hz), which is slow compared with the resolution of EEG/magnetoencephalography (MEG). Newly developed fast fMRI techniques can reach a temporal resolution of 500 ms, so that the effect of biophysical noises (e.g., cardiach and respiration) can be largely reduced. Moreover, future studies based on multimodal neuroimaging, including EEG/MEG or electrocorticography together with fMRI, would better delineate the potential bioelectrical mechanism that underlies dFC.

Conclusion

The dFC analytic method reliably assesses changes in amygdala connectivity, and the impaired positive/negative dFC that we found in untreated patients with first-episode MDD involved amygdala structures, the superior prefrontal gyrus and the thalamus. Thus, the limbic–cortical–striato–pallido–thalamic circuit likely plays an important role in the early stages of MDD. The abnormal connection of amygdalar subregions might provide a neural-network explanation for depressive symptoms, including negative bias, impaired social cognition and diminished motivational and behavioural responses. Because the structure and function of the amygdala may be altered in a state-dependent manner, additional investigation is needed to determine whether our results regarding amygdalar subregion dFC change represent a trait or a state marker. Future longitudinal research is needed to understand how amygdalar subregion dFC changes during MDD development, over the course of illness, and with treatment response, and to further examine the relationships between these changes and symptom dimensions.

Acknowledgments: This work was supported by the Natural Science Foundation of China (grant nos. 81401479, 81671767, 91432115, 81225012, 81621003, 81220108013, 81227002, 81620108016, 31521063 and 81030027), the Beijing Natural Science Foundation (grant nos. Z151100003915082, Z161100000216125 and Z161100000216152), the Fundamental Research Funds for the Central Universities (grant nos. 2015KJCA13 and 2017XTCX04), the Chinese Postdoctoral Science Foundation (grant no. 2015M582554), the Changjiang Scholar Professorship Award (award no. T2015027 and T2014190) and the Sichuan Provincial Health and Family Planning Commission (grant no. 150251). Q. Gong also acknowledges the support provided by his CMB Distinguished Professorship Award (award no. F510000/G16916411) administered by the Institute of International Education, USA.

Affiliations: From the Huaxi MR Research Centre (HMRRCC), Department of Radiology, West China Hospital of Sichuan University, Chengdu, Sichuan, China (Qiu, Chen, Lui, Huang, Gong); the Department of Radiology, The Second People's Hospital of Yibin, Yibin, China (Qiu); the National Key Laboratory of Cognitive Neuroscience and Learning, Beijing Normal University, Beijing, China (Xia, Yuan, He); the Beijing Key Laboratory of Brain Imaging and Connectomics, Beijing Normal University, Beijing, China (Xia, He); the IDG/McGovern Institute for Brain Research, Beijing Normal University, Beijing, China (Xia, He); the Department of Psychiatry, State Key Lab of Biotherapy, West China Hospital, Sichuan University, Chengdu, Sichuan, China (Kuang); the Department of Oncology, State Key Lab of Biotherapy, West China Hospital, Sichuan University, Chengdu, Sichuan, China (Bi); the National Engineering Research Centre for Biomaterials, Sichuan University, Chengdu, Sichuan, China (Ai, Gu).

Competing interests: None declared.

Contributors: All authors designed the study. L. Qiu and B. Cheng acquired the data, which L. Qiu and M. Xia analyzed. L. Qiu and M. Xia wrote the article, which all authors reviewed. All authors approved the final version to be published and can certify that no other individuals not listed as authors have made substantial contributions to the paper.

References

- Price JL, Drevets WC. Neurocircuitry of mood disorders. *Neuropsychopharmacology* 2010;35: 192-216.
- LeDoux JE. Emotion circuits in the brain. *Annu Rev Neurosci* 2000;23:155-84.
- Pessoa L. On the relationship between emotion and cognition. *Nat Rev Neurosci* 2008;9:148-58.
- van Eijndhoven P, van Wingen G, van Oijen K, et al. Amygdala volume marks the acute state in the early course of depression. *Biol Psychiatry* 2009;65:812-8.
- Frodl T, Meisenzahl EM, Zetsche T, et al. Larger amygdala volumes in first depressive episode as compared to recurrent major depression and healthy control subjects. *Biol Psychiatry* 2003; 53:338-44.
- Hamilton JP, Siemer M, Gotlib IH. Amygdala volume in major depressive disorder: a meta-analysis of magnetic resonance imaging studies. *Mol Psychiatry* 2008;13:993-1000.
- Sheline YI, Barch DM, Price JL, et al. The default mode network and self-referential processes in depression. *Proc Natl Acad Sci U S A* 2009;106:1942-7.
- Yoshimura S, Ueda K, Suzuki S, et al. Self-referential processing of negative stimuli within the ventral anterior cingulate gyrus and right amygdala. *Brain Cogn* 2009;69:218-25.
- Cullen KR, Westlund MK, Klimes-Dougan B, et al. Abnormal amygdala resting-state functional connectivity in adolescent depression. *JAMA Psychiatry* 2014;71:1138-47.
- Connolly CG, Ho TC, Blom EH, et al. Resting-state functional connectivity of the amygdala and longitudinal changes in depression severity in adolescent depression. *J Affect Disord* 2017;207:86-94.
- Jones DT, Vemuri P, Murphy MC, et al. Non-stationarity in the "resting brain's" modular architecture. *PLoS ONE* 2012;7:e39731.
- Sakoglu U, Pearlson GD, Kiehl KA, et al. A method for evaluating dynamic functional network connectivity and task-modulation: application to schizophrenia. *MAGMA* 2010;23:351-66.
- Kaiser RH, Whitfield-Gabrieli S, Dillon DG, et al. Dynamic resting-state functional connectivity in major depression. *Neuropsychopharmacology* 2016;41:1822-30.
- Demirtas M, Tornador C, Falcon C, et al. Dynamic functional connectivity reveals altered variability in functional connectivity among patients with major depressive disorder. *Hum Brain Mapp* 2016;37:2918-30.
- Peng D, Shi F, Shen T, et al. Altered brain network modules induce helplessness in major depressive disorder. *J Affect Disord* 2014; 168:21-9.
- Li W, Ward BD, Xie C, et al. Amygdala network dysfunction in late-life depression phenotypes: relationships with symptom dimensions. *J Psychiatr Res* 2015;70:121-9.
- Amunts K, Kedo O, Kindler M, et al. Cytoarchitectonic mapping of the human amygdala, hippocampal region and entorhinal cortex: intersubject variability and probability maps. *Anat Embryol (Berl)* 2005;210:343-52.
- Saygin ZM, Osher DE, Augustinack J, et al. Connectivity-based segmentation of human amygdala nuclei using probabilistic tractography. *Neuroimage* 2011;56:1353-61.
- Bzdok D, Laird AR, Zilles K, et al. An investigation of the structural, connective, and functional subspecialization in the human amygdala. *Hum Brain Mapp* 2013;34:3247-66.
- Etkin A, Prater KE, Schatzberg AF, et al. Disrupted amygdalar subregion functional connectivity and evidence of a compensatory network in generalized anxiety disorder. *Arch Gen Psychiatry* 2009;66:1361-72.
- Roy AK, Shehzad Z, Margulies DS, et al. Functional connectivity of the human amygdala using resting state fMRI. *Neuroimage* 2009;45:614-26.
- Phelps EA, LeDoux JE. Contributions of the amygdala to emotion processing: from animal models to human behavior. *Neuron* 2005;48:175-87.
- LeDoux J. The emotional brain, fear, and the amygdala. *Cell Mol Neurobiol* 2003;23:727-38.
- Davis M. Neurobiology of fear responses: the role of the amygdala. *J Neuropsychiatry Clin Neurosci* 1997;9:382-402.
- Sah P, Faber ES, Lopez De Armentia M, et al. The amygdaloid complex: anatomy and physiology. *Physiol Rev* 2003;83:803-34.
- Ubeda-Banon I, Novejarque A, Mohedano-Moriano A, et al. Projections from the posterolateral olfactory amygdala to the ventral striatum: neural basis for reinforcing properties of chemical stimuli. *BMC Neurosci* 2007;8:103.
- Kerestes R, Chase HW, Phillips ML, et al. Multimodal evaluation of the amygdala's functional connectivity. *Neuroimage* 2017;148: 219-29.

28. Yu X, Liu L, Chen W, et al. Integrity of amygdala subregion-based functional networks and emotional lability in drug-naive boys with ADHD. *J Atten Disord* 2016;1087054716661419.
29. Roy AK, Fudge JL, Kelly C, et al. Intrinsic functional connectivity of amygdala-based networks in adolescent generalized anxiety disorder. *J Am Acad Child Adolesc Psychiatry* 2013; 52:290-9, e2.
30. Doucet GE, Skidmore C, Sharan AD, et al. Functional connectivity abnormalities vary by amygdala subdivision and are associated with psychiatric symptoms in unilateral temporal epilepsy. *Brain Cogn* 2013;83:171-82.
31. Kleinhans NM, Reiter MA, Neuhaus E, et al. Subregional differences in intrinsic amygdala hyperconnectivity and hypoconnectivity in autism spectrum disorder. *Autism Res* 2016;9: 760-72.
32. First MB, Spitzer RL, Miriam G, et al. Structured clinical interview for DSM-IV axis I disorders: SCID-I: clinical version: administration booklet. Washington (DC): American Psychiatric Press, 1997.
33. Williams JB. A structured interview guide for the Hamilton Depression Rating Scale. *Arch Gen Psychiatry* 1988;45:742-7.
34. Chao-Gan Y, Yu-Feng Z. DPARSF: A MATLAB toolbox for "pipeline" data analysis of resting-state fMRI. *Front Syst Neurosci* 2010;4:13.
35. Friston KJ, Williams S, Howard R, et al. Movement-related effects in fMRI time-series. *Magn Reson Med* 1996;35:346-55.
36. Zilles K, Amunts K. Centenary of Brodmann's map—conception and fate. *Nat Rev Neurosci* 2010;11:139-45.
37. Eickhoff SB, Stephan KE, Mohlberg H, et al. A new SPM toolbox for combining probabilistic cytoarchitectonic maps and functional imaging data. *Neuroimage* 2005;25:1325-35.
38. Allen EA, Damaraju E, Plis SM, et al. Tracking whole-brain connectivity dynamics in the resting state. *Cereb Cortex* 2014;24:663-76.
39. Zalesky A, Fornito A, Cocchi L, et al. Time-resolved resting-state brain networks. *Proc Natl Acad Sci U S A* 2014;111:10341-6.
40. Eklund A, Nichols TE, Knutsson H. Cluster failure: Why fMRI inferences for spatial extent have inflated false-positive rates. *Proc Natl Acad Sci U S A* 2016;113:7900-5.
41. Fransson P. Spontaneous low-frequency BOLD signal fluctuations: an fMRI investigation of the resting-state default mode of brain function hypothesis. *Hum Brain Mapp* 2005;26:15-29.
42. Fox MD, Zhang D, Snyder AZ, et al. The global signal and observed anticorrelated resting state brain networks. *J Neurophysiol* 2009;101:3270-83.
43. Birn RM, Diamond JB, Smith MA, et al. Separating respiratory-variation-related fluctuations from neuronal-activity-related fluctuations in fMRI. *Neuroimage* 2006;31:1536-48.
44. Murphy K, Birn RM, Handwerker DA, et al. The impact of global signal regression on resting state correlations: are anti-correlated networks introduced? *Neuroimage* 2009;44:893-905.
45. Weissenbacher A, Kasess C, Gerstl F, et al. Correlations and anti-correlations in resting-state functional connectivity MRI: a quantitative comparison of preprocessing strategies. *Neuroimage* 2009;47:1408-16.
46. Power JD, Barnes KA, Snyder AZ, et al. Spurious but systematic correlations in functional connectivity MRI networks arise from subject motion. *Neuroimage* 2012;59:2142-54.
47. Satterthwaite TD, Wolf DH, Loughhead J, et al. Impact of in-scanner head motion on multiple measures of functional connectivity: relevance for studies of neurodevelopment in youth. *Neuroimage* 2012;60:623-32.
48. Van Dijk KR, Sabuncu MR, Buckner RL. The influence of head motion on intrinsic functional connectivity MRI. *Neuroimage* 2012;59:431-8.
49. Zeng LL, Wang D, Fox MD, et al. Neurobiological basis of head motion in brain imaging. *Proc Natl Acad Sci U S A* 2014;111:6058-62.
50. Hutchison RM, Womelsdorf T, Allen EA, et al. Dynamic functional connectivity: promise, issues, and interpretations. *Neuroimage* 2013;80:360-78.
51. Kiviniemi V, Vire T, Remes J, et al. A sliding time-window ICA reveals spatial variability of the default mode network in time. *Brain Connect* 2011;1:339-47.
52. Price JL. Comparative aspects of amygdala connectivity. *Ann N Y Acad Sci* 2003;985:50-8.
53. Medina JF, Repa JC, Mauk MD, et al. Parallels between cerebellum- and amygdala-dependent conditioning. *Nat Rev Neurosci* 2002; 3:122-31.
54. Heimer L, Van Hoesen GW. The limbic lobe and its output channels: implications for emotional functions and adaptive behavior. *Neurosci Biobehav Rev* 2006;30:126-47.
55. Gonzalez-Lima F, Scheich H. Classical conditioning of tone-signaled bradycardia modifies 2-deoxyglucose uptake patterns in cortex, thalamus, habenula, caudate-putamen and hippocampal formation. *Brain Res* 1986;363:239-56.
56. Kempainen S, Jolkonen E, Pitkanen A. Projections from the posterior cortical nucleus of the amygdala to the hippocampal formation and parahippocampal region in rat. *Hippocampus* 2002;12:735-55.
57. Song YJ, Korgaonkar MS, Armstrong LV, et al. Tractography of the brainstem in major depressive disorder using diffusion tensor imaging. *PLoS ONE* 2014;9:e84825.
58. Russchen FT, Amaral DG, Price JL. The afferent input to the magnocellular division of the mediodorsal thalamic nucleus in the monkey, *Macaca fascicularis*. *J Comp Neurol* 1987;256:175-210.
59. Bubser M, Deutch AY. Stress induces Fos expression in neurons of the thalamic paraventricular nucleus that innervate limbic fore-brain sites. *Synapse* 1999;32:13-22.
60. Critchley HD, Elliott R, Mathias CJ, et al. Neural activity relating to generation and representation of galvanic skin conductance responses: a functional magnetic resonance imaging study. *J Neurosci* 2000;20:3033-40.
61. Williams LM, Brammer MJ, Skerrett D, et al. The neural correlates of orienting: an integration of fMRI and skin conductance orienting. *Neuroreport* 2000;11:3011-5.
62. Teves D, Videen TO, Cryer PE, et al. Activation of human medial prefrontal cortex during autonomic responses to hypoglycemia. *Proc Natl Acad Sci U S A* 2004;101:6217-21.
63. Likhtik E, Pelletier JG, Paz R, et al. Prefrontal control of the amygdala. *J Neurosci* 2005;25:7429-37.
64. Perez-Jaranay JM, Vives F. Electrophysiological study of the response of medial prefrontal cortex neurons to stimulation of the basolateral nucleus of the amygdala in the rat. *Brain Res* 1991;564:97-101.
65. Garrett DD, Kovacevic N, McIntosh AR, et al. Blood oxygen level-dependent signal variability is more than just noise. *J Neurosci* 2010;30:4914-21.
66. Garrett DD, Kovacevic N, McIntosh AR, et al. The importance of being variable. *J Neurosci* 2011;31:4496-503.
67. Garrett DD, McIntosh AR, Grady CL. Brain signal variability is parametrically modifiable. *Cereb Cortex* 2014;24:2931-40.
68. McIntosh AR, Kovacevic N, Itier RJ. Increased brain signal variability accompanies lower behavioral variability in development. *PLoS Comput Biol* 2008;4:e1000106.
69. Lui S, Zhou XJ, Sweeney JA, et al. Psychoradiology: the frontier of neuroimaging in psychiatry. *Radiology* 2016;281:357-72.